Published as *International Journal of Thermophysics* **33**, 1488-1499 (2012).

Uncertainty Budget for the NIST Hybrid Humidity Generator

C. W. Meyer[1], W. W. Miller, D. C. Ripple, and G. E. Scace

Process Measurements Division, National Institute of Standards and Technology, Gaithersburg, Maryland 20899, U.S.A.

[1] To whom correspondence should be addressed. E-mail: cmeyer@nist.gov

ABSTRACT

We provide here a detailed uncertainty budget for the new Hybrid Humidity Generator (HHG) that has been constructed at the National Institute of Standards and Technology. The HHG generates frost/dew points from –70 °C to +85 °C using calibration gas flows up to 150 L/min. For frost/dew points above –15 °C, the two-pressure method is employed, and for frost points at or below –15 °C, the divided-flow method is used (hence the name "hybrid"). The total expanded (k=2) uncertainty is estimated for HHG generation of the following quantities: frost/dew point, mole fraction, and relative humidity. The total uncertainty is estimated separately for the two-pressure and divided-flow methods.

KEY WORDS: humidity; generator; standards; saturator; calibration; hygrometer; uncertainty; water vapor.

1. INTRODUCTION

The National Institute of Standards and Technology (NIST) has constructed a new primary standard humidity generator [1−3]. The facility is called the Hybrid Humidity Generator (HHG), and is so named because it incorporates the two-pressure and divided-flow humidity-generation methods [4] into a single design. For frost/dew points from –15 °C to 85 °C, we employ the two-pressure method, and for frost points from –70 °C to –15 °C, we use the divided-flow method. The design of the HHG is novel, as it is the first primary generator design that incorporates the divided-flow method. It is now NIST's principal standard humidity generator for calibration of customer hygrometers. The NIST Low Frost-point Generator (LFPG) [5] operates as a complement to the HHG and is used for calibration of hygrometers requiring frost points below −70 °C. The HHG accommodates gas flows up to 150 L/min. Currently, the HHG only calibrates hygrometers that do not require a calibration test chamber, but this will change once the newly constructed HHG test chamber has been adequately characterized.

We provide here a detailed uncertainty budget for the HHG (excluding the test chamber). The total expanded (k=2) uncertainty is estimated for HHG generation of the following quantities: frost/dew point, mole fraction, and relative humidity. The relative humidity uncertainty assumes calibration of a chilled-mirror hygrometer with an external temperature probe, as such a calibration does not require a test chamber. The total uncertainty is estimated separately for the cases of two-pressure mode and divided-flow mode. First we present a table listing all the uncertainty elements and their estimated uncertainty values. Then we provide equations relating the total uncertainty of each quantity to the uncertainty elements and plot this uncertainty.

2. GENERATOR DESIGN

The design of the generator is described in full detail elsewhere [1,3], so we provide only a brief description here. A schematic representation of the layout of the HHG is shown in Fig. 1 for the a) two-pressure and b) divided-flow method. The system includes a dry-gas source, a two-pressure saturation system and a dilution system.

The gas used in the HHG comes from the in-house supply of compressed air at NIST. Before entering the generator, the gas, regulated by mass flow controllers, passes through a large regenerating gas dryer and CO_2 scrubber.

The saturation system of the HHG consists of a pre-saturator and final saturator. The pre-saturator accomplishes virtually all of the saturation and the final saturator performs small adjustments. The stainless-steel final saturator, shown in Figure 2, is composed of a heat exchanger located immediately above a saturation chamber. Both systems rest inside a temperature-controlled bath. The heat exchanger brings the temperature of the incoming gas to within 1 mK of the saturation-chamber temperature. The heat exchanger consists of two header tanks separated by an array of parallel tubes. The saturation chamber contains a layer of water and a layer of gas above it. Dividers inside the saturator partition the chamber into two, equal-area channels that follow a serpentine path.

The mole fraction x of water vapor in the exiting gas is then calculated using the equation

$$x = \frac{e_w(T_s)}{P_s} f(T_s, P_s) \qquad 1)$$

Here, T_s and P_s are the temperature and pressure of the gas and water in the saturator, and $e_w(T_s)$ is the water vapor pressure at T_s as calculated by [6,7]. The enhancement factor $f(T_s, P_s)$ reflects departures from ideal solution behaviour and non-ideal gas effects [8].

We measure the temperature of the saturator using a standard platinum resistance thermometer (SPRT) immersed in the temperature-controlled bath. Silicon strain gauges measure the saturator pressure and the "chamber" pressure P_c downstream of the saturation chamber (for frost/dew point and relative humidity determination).

The two-pressure technique [4] saturates the gas at P_s (usually elevated) and afterwards lowers the pressure of the gas (if necessary) down to P_c. In the HHG, the saturator may be pressurized up to 550 kPa; the gas then exits through an expansion valve that controls the saturator pressure by adjusting the gas flow rate out of the saturator. When using the two-pressure technique, the mole fraction can be changed to the desired value by either changing P_s or T_s (see Eq. 1). Changing P_s, which is faster than changing T_s, allows faster calibration of hygrometers over a range of humidity values. In the two-pressure method, when the HHG is operated with the expansion valve completely open ($P_s \approx P_c$), it is said to be operating in "1-P mode", and when it is operated with $P_s > P_c$, it is said to be operating in "2-P mode". In practice, the lowest value of P_s used in the 2-P mode is P_s = 125 kPa. During a calibration, the operator typically generates the highest desired mole fraction using 1-P mode. Afterwards, P_s is increased (2-P mode) to lower the generated mole fraction to the next calibration point. For subsequent points, P_s is continually increased until the required value of P_s is above 500 kPa. In this case, the 1-P mode is used for the next calibration point, and the sequence continues until the calibration is finished or the bottom of the two-pressure range is reached.

The divided-flow method [4] (used for generating frost points at or less than −15 °C) involves diluting the saturated gas with dry gas using precisely metered streams of gas. The mole fraction after dilution is

$$x = \frac{\dot{n}_s x_s + \dot{n}_p x_p}{\dot{N}} \qquad 2)$$

where $\dot{n}_s$ and $\dot{n}_p$ are the molar flow rates of the saturated gas and pure gas, respectively, and $\dot{N}$ is the total molar flow rate. Also, x_s is the mole fraction of water in the saturated gas and x_p is the residual mole fraction of water in the pure gas. This allows generation of arbitrarily low humidity values while operating the saturator at convenient temperatures. References [1,3] describe the design of the divided flow system for the HHG. When operated with this method and with a saturator pressure of 300 kPa, the HHG is said to be operating in "divided-flow mode".

The dew-point temperature T_{DP} and frost-point temperature T_{FP} are obtained from the mole fraction by iteratively solving the equations

$$x = \frac{e_w(T_{DP})}{P_c} f(T_{DP}, P_c) \quad \text{and} \quad x = \frac{e_i(T_{FP})}{P_c} f(T_{FP}, P_c), \tag{3}$$

where $e_w(T_{DP})$ and $e_i(T_{FP})$ are the saturated vapor pressures of water and ice at the dew point and the frost point, respectively. The relative humidity is determined by

$$RH = \frac{xP_c}{e(T_c) f(T_c, P_c)}, \tag{4}$$

where T_c is the temperature in the chamber (or environment) where the humidity is being determined, and $e(T_c) = e_w(T_c)$ for $T_c \geq 0$ °C and $e(T_c) = e_i(T_c)$ for $T_c < 0$ °C.

3. UNCERTAINTY BUDGET

We have constructed an uncertainty budget for the humidity generated by the HHG, based on the ISO and NIST guidelines for the expression of uncertainty in measurement [9,10]. We present here the total uncertainty for water mole fraction, frost/dew point, and relative humidity. For these quantities, we present the uncertainty for the cases of humidity generated using the two-pressure principle (for both 1-P and 2-P modes) and divided-flow method. In

this analysis, $u(X)$ is the standard uncertainty of the quantity X. The equations presented here are derived in Appendix I of [3]. In the equations, the following abbreviations are made: $e_s \equiv e_w(T_s)$ and $f_s \equiv f(T_s,P_s)$. Also, for dew point uncertainties, $e_c \equiv e_w(T_{DP})$, and $f_c \equiv f(T_{DP},P_c)$ and for frost point uncertainties, $e_c \equiv e_i(T_{FP})$, and $f_c \equiv f(T_{FP},P_c)$. Finally, for relative humidity uncertainties, $e_c \equiv e(T_c)$, and $f_c \equiv f(T_c,P_c)$.

Shown in Table 1 are all the relevant uncertainty elements mentioned above and their standard uncertainty values. The subcomponents of the uncertainty elements T_s, P_s, and P_c are given in Appendix II of [3]. These subcomponents, along with the uncertainties $\dot{n}_s$ and $\dot{n}_p$, and x_p are based on performance tests [2], calibration uncertainties, and equipment manufacturer specifications. The value for the uncertainty of T_c is based on the typical uncertainty for the calibration of external temperature probes at NIST [11]. Also, $u\left(e_s^{calc}\right)$, $u\left(e_c^{calc}\right)$, $u\left(f_s^{calc}\right)$ and $u\left(f_c^{calc}\right)$ are the uncertainties of the calculated values of $e(T_s)$, $e(T_c)$, $f(T_s,P_s)$, and $f(T_s,P_s)$, respectively, due to the imperfect knowledge of these physical relations [12,13,14]. The relative uncertainties $u\left(e_s^{calc}\right)/\left(e_s^{calc}\right)$ and $u\left(e_c^{calc}\right)/\left(e_c^{calc}\right)$ for $T_c \geq 0$ °C are obtained from the maximum 1σ relative uncertainty value in Table 2 of [12]; for simplicity we have chosen to keep these relative uncertainties constant rather than include their actual temperature dependence. The uncertainty $u\left(e_c^{calc}\right)$ for $T_c < 0$ °C, which is plotted in [13], is obtained from [14]. Since [14] contains the full uncertainty equation and is not yet in print, a quadratic fit to this equation, good to 5 parts in 10^6, is provided in Table 1. The uncertainties $u\left(f_s^{calc}\right)$ and $u\left(f_c^{calc}\right)$ are presented as a fit to the uncertainty data of Table 9 in [15]; because there is no data below −50 °C, we extrapolated the curve determined from the available data to obtain the uncertainty formula listed in Table 1. In obtaining the formula, the "maximum percentage uncertainties" from [15] were divided by $\sqrt{3}$ to obtain the standard uncertainty.

3.1 Water Mole Fraction Generated Using the Two-Pressure Method. Here, the total standard uncertainty for the water mole fraction, $u(x)$, is expressed as

$$u(x)^2 = \left(\frac{1}{P_s}\frac{de_s}{dT_s}\right)^2 u(T_s)^2 + \left(\frac{e_s}{P_s^2}\right)^2 u(P_s)^2 + \left(\frac{1}{P_s}\right)^2 u\left(e_s^{\text{calc}}\right)^2 + \left(\frac{e_s}{P_s}\right)^2 u\left(f_s^{\text{calc}}\right)^2 . \quad 5)$$

Figure 3 shows the total expanded relative uncertainty and its components for the mole fraction generated by the HHG using the two pressure principle in a) 1-P mode and b) 2-P mode with P_s = 500 kPa. Here, the total expanded relative uncertainty is given by $U_r(x) = ku(x)/x$, where the coverage factor is $k = 2$. The uncertainty is generally lowest for the 1-P mode and highest for the 2-P mode with P_s = 500 kPa. For simplicity, we generally use the latter for representing the HHG uncertainty when using the two-pressure principle.

3.2 Frost/dew Point Using the Two-Pressure Method. Here, the total standard uncertainty for T_{DP} in a gas with pressure P_c is obtained by considering the gas to be in a hypothetical chamber with temperature $T_c = T_{DP}$. The uncertainty is then expressed as

$$u(T_{DP})^2 = \left(\frac{e_c}{[de_c/dT_c]}\right)^2 \left[\left(\frac{1}{e_s}\frac{de_s}{dT_s}\right)^2 u(T_s)^2 + \frac{u(P_s)^2}{P_s^2} + \frac{u(P_c)^2}{P_c^2} + u\left(\Delta f^{\text{calc}}\right)^2 + u_r\left(\Delta e^{\text{calc}}\right)^2\right] \quad 6)$$

In Eq. 6, the last two terms reflect uncertainties in the changes of f^{calc} and e^{calc} when the temperature/pressure combination is changed from T_s,P_s to T_{DP},P_c. When the generator is used in 1-P mode ($P_c \cong P_s$, $T_{DP} \cong T_s$), we approximate

$$u_r\left(\Delta e^{\text{calc}}\right) \cong u\left(\Delta f^{\text{calc}}\right) \cong 0 . \quad 7)$$

When the generator is used in 2-P mode ($P_s \neq P_c$), we approximate

$$u_r\left(\Delta e^{\text{calc}}\right)^2 \cong \frac{u\left(e_s^{\text{calc}}\right)^2}{e_s^2} + \frac{u\left(e_c^{\text{calc}}\right)^2}{e_c^2} , \quad 8)$$

$$u\left(\Delta f^{\text{calc}}\right)^2 \cong u\left(f_s^{\text{calc}}\right)^2 + u\left(f_c^{\text{calc}}\right)^2 . \quad 9)$$

The standard uncertainty of the frost point, $u(T_{FP})$, is given by Eq. 6, substituting "DP" with "FP". Figure 4 shows the total expanded uncertainty and its components for the frost/dew

point generated by the HHG using the two pressure principle in a) 1-P mode and b) 2-P mode with P_s = 500 kPa. Here, the total expanded uncertainty is given by $U(x) = ku(x)$. In Fig. 4(a), the uncertainty contributions from e_s^{calc} and e_c^{calc} are zero, because these uncertainties cancel out when the generator is used in 1-P mode; the uncertainty contributions for f_s^{calc} and f_c^{calc} are zero for the same reason. The figure shows that for the 1-P mode, the dominant uncertainty is from pressure measurement and instability, except for saturator temperatures above 60 °C; in this case uncertainties due to temperature non-uniformities in the bath dominate. In Fig. 4(b), the discontinuity at 0 °C is due to the assumption of frost condensation below this temperature and the resulting discontinuity in $e_c/[de_c/dT_c]$. This figure shows that when the saturator is operated in 2-P mode, the uncertainties in f_s^{calc} and f_c^{calc} usually dominate and raise considerably the total uncertainty.

3.3 Relative Humidity Generated Using the Two-pressure Method. The total standard uncertainty for relative humidity $u(RH)$ of the gas in a test chamber with temperature T_c and pressure P_c is expressed as

$$u(RH)^2 = \left[\frac{P_c e_s}{P_s e_c}\right]^2 \left[\left(\frac{1}{e_s}\frac{de_s}{dT_s}\right)^2 u(T_s)^2 + \frac{1}{P_s}u(P_s)^2 + \left(\frac{1}{e_c}\frac{de_c}{dT_c}\right)^2 u(T_c)^2 + \frac{1}{P_c}u(P_c)^2 + u\left(\Delta e^{calc}\right)^2 + u\left(\Delta f^{calc}\right)^2\right] \quad (10)$$

Here, $u\left(\Delta e^{calc}\right)$ and $u\left(\Delta f^{calc}\right)$ are given by Eqs. 7−8. Figure 5 shows the expanded relative uncertainty $U_r(RH) = U(RH)/RH$ for relative humidity calibrations using humid gas generated by the HHG and flowing to an environment with temperature T_c = 20 °C and pressure 100 kPa. Here, $U_r(RH)$ includes the uncertainty of the humidity produced by the generator and the uncertainty of the calibration of the hygrometer's external temperature probe. In the figure the generator is operated in 2-P mode; the plots show the uncertainty for two saturator temperatures: a) T_s = 20 °C and b) T_s = 1 °C, which generate different relative humidity ranges.

3.4 Water Mole Fraction Generated in Divided-flow Mode. For this case, $u(x)$ is expressed as

$$u(x)^2 \cong x^2\left[\left(\frac{1}{e_s}\frac{de_s}{dT_s}\right)^2 u(T_s)^2 + \frac{u(P_s)^2}{P_s{}^2} + \frac{u\left(e_s^{calc}\right)^2}{e_s{}^2} + u\left(f_s^{calc}\right)^2 + \frac{u(\dot{n}_p)^2}{\dot{N}^2} + \left(\frac{x_s}{x}-1\right)^2\left(\frac{u(x_p)^2}{x_s{}^2} + \frac{u(\dot{n}_s)^2}{\dot{N}^2}\right)\right] \quad (11)$$

Figure 6 shows the expanded relative uncertainty of the water mole fraction generated by the HHG when it is used in divided-flow mode. The saturator parameters are P_s = 300 kPa and T_s = 0.5 °C. In the plot, "*n*" refers to the combined contribution to the total from $\dot{n}_s$ and $\dot{n}_p$. In the figure, $U_r(x)$ is relatively constant for $x > 2\times10^{-5}$. At the highest value of x shown in the plot, $\dot{n}_p = 0$ and so $U_r(x)$ is only due to the saturator. As x decreases to 2×10^{-5}, $U_r(x)$ increases slightly due to the rising significance of $u(\dot{n}_s)$ and $u(\dot{n}_p)$. As x decreases below 2×10^{-5}, $u(x_p)/x$ dominates $U_r(x)$, increasing its value to nearly 0.8 % at $x = 2.5\times10^{-6}$.

3.5 Frost Point Generated in Divided-flow Mode. In the hybrid generator, the divided flow method will only be used for generating frost points. Here, the total standard uncertainty of T_{FP} in a gas with pressure P_c is obtained by considering the gas to be in a hypothetical chamber with temperature $T_c = T_{FP}$. The uncertainty is then

$$u(T_{FP})^2 = \frac{(xP_c)^2}{\left[de_c/dT_c\right]^2}\left[\left(\frac{1}{e_s}\frac{de_s}{dT_s}\right)^2 u(T_s)^2 + \frac{u(P_s)^2}{P_s{}^2} + \left(\frac{x_s}{x}-1\right)^2\left(\frac{u(x_p)^2}{x_s{}^2} + \frac{u(\dot{n}_s)^2}{\dot{N}^2}\right) + \frac{u(\dot{n}_p)^2}{\dot{N}^2} + \frac{u(P_c)^2}{P_c{}^2} + \frac{u\left(e_s^{calc}\right)^2}{e_s{}^2} + \frac{u\left(e_c^{calc}\right)^2}{(xP_c)^2} + u\left(\Delta f^{calc}\right)^2\right] \quad (12)$$

Here, $u\left(\Delta f^{calc}\right)$ is defined in Eq. 9. Figure 7 shows the expanded uncertainty of the frost point generated by the HHG when it is used in divided-flow mode. Here, the total expanded uncertainty is $U(T_{FP}) = ku(T_{FP})$. For −55 °C ≤ T_{FP} ≤ −12 °C, $U(T_{FP})$ ≈ 20 mK and is relatively

constant over this entire range. As T_{FP} decreases below −55 °C, $U(T_{FP})$ rises rapidly up to 58 mK at −70 °C due to the increasing influence of $u(x_p)$.

3.6 Relative Humidity Generated in Divided-flow Mode. Here, the total standard uncertainty of the relative humidity of the gas in the test chamber is

$$u(RH)^2 = \left[\frac{xP_c}{e_c}\right]^2 \left[\left(\frac{1}{e_s}\frac{de_s}{dT_s}\right)^2 u(T_s)^2 + \frac{u(P_s)^2}{P_s^{\,2}} + \frac{u\left(e_s^{\,calc}\right)^2}{e_s^{\,2}} + u\left(f_s^{\,calc}\right)^2 + \left(\frac{x_s}{x} - 1\right)^2 \left(\frac{u(x_p)^2}{x_s^{\,2}} + \frac{u(\dot{n}_s)^2}{\dot{N}^2}\right) + \frac{u(\dot{n}_p)^2}{\dot{N}^2}\right] + \left(\frac{P_c}{e_c}\right)^2 \left(x + \frac{\dot{n}_p}{\dot{N}} x_p\right)^2 \left[\frac{u(P_c)^2}{P_c^{\,2}} + \left(\frac{1}{e_c}\frac{de_c}{dT_c}\right)^2 u(T_c)^2 + \frac{u(e_c^{\,calc})^2}{e_c^{\,2}} + u(f_c^{\,calc})^2\right] \quad (13)$$

Figure 8 shows $U_r(RH)$ for relative humidity calibrations using humid gas generated by the HHG using the divided-flow method and flowing to an environment with temperature T_c = 20 °C and pressure 100 kPa.

4. SUMMARY

We have described here the uncertainty of the new hybrid generator at NIST, which generates frost/dew points between −70 °C and 85 °C (mole fractions between 2.5 μmol/mol and 0.57 mol/mol). Between −60 °C and 85 °C the frost/dew point expanded uncertainty is always below 25 mK. Between −70 °C and −60 °C the uncertainty is between 25 mK and 60 mK. For mole fraction, $U_r(x) < 0.2$ % for $x \geq 20$ μmol/mol. As x decreases below this value, $U_r(x)$ increases to 0.8 % at 2.5 μmol/mol.

ACKNOWLEDGMENTS

The authors gratefully thank Joseph Hodges and Jon Hougen for useful comments on the manuscript.

REFERENCES

1. G.E. Scace et al., in *Proceedings of the 5th International Symposium on Humidity and Moisture* (Rio de Janeiro, Brazil: INMETRO, 2007).
2. C.W. Meyer et al, in *Proceedings of the 10th International Symposium on Temperature and Thermal Measurements in Industry and Science (TEMPMEKO 2007),* Int. J. Thermophys. **29**, 1606 (2007).
3. C.W. Meyer et al, NIST Special Publication 250-83 (2008).
4. A. Wexler, *Tappi* **44**,180A (1961).
5. G.E. Scace et al., in *Papers and Abstracts from the Third International Symposium on Humidity and Moisture*, (Teddington, UK: National Physical Laboratory, 1998), pp. 180−190.
6. A. Saul and W. Wagner, *J. Phys. Chem. Ref. Data* **16**, 893 (1987).
7. W. Wagner and A. Pruss, *J. Phys. Chem. Ref. Data* **22**, 783 (1993).
8. R.W. Hyland and A. Wexler, *ASHRAE Trans.* **89-IIa**, 520 (1983).
9. ISO, Guide to the Expression of Uncertainty in Measurement, International Organization for Standardization, Geneva (1993).
10. B.N. Taylor and C.E. Kuyatt, NIST Technical Note 1297, National Institute of Standards and Technology, Gaithersburg (1994).
11. C.D. Vaughn and G.F. Strouse, The NIST Industrial Thermometer Calibration Laboratory, in *Proceedings of TEMPMEKO 2001: the 8th International Symposium on Temperature and Thermal Measurements*, B. Fellmuth, J. Seidel, G. Scholz, eds., (VDE Verlag GMBH, Berlin, 2002), pp. 629-634.
12. A. Wexler, *Jour. Res. NBS* **80A,** 775 (1976).
13. International Association for the Properties of Water and Steam, *Revised Release on the Pressure along the Melting and Sublimation Curves of Ordinary Water Substance* (2008), available at www.iapws.org.
14. W. Wagner, Riethmann, R. Feistel, and A.H. Harvey, to be submitted to *J. Phys. Chem. Ref. Data*.

15. R.W. Hyland, *Jour. Res. NBS* **79A,** 551 (1975).

Table 1. Uncertainty elements for the Hybrid Humidity Generator and their uncertainties. Here, $u(X)$ is the standard uncertainty for element X. The elements with subscript "c" refer to the environment in which the humidity is to be determined. The element T_c is only relevant when the hygrometer uses an external thermometer for determination of relative humidity.

X	$u(X)$ $(k = 1)$	Condition	Unit
T_s	1.5	($T \leq 40$ °C)	mK
	$0.16 T_s$/°C – 4.9	($T > 40$ °C)	
P_s	18	($P_s \approx$ ambient pressure)	Pa
	$\sqrt{29^2 + (P_s/10000\ \text{Pa})^2}$	($P_s >$ ambient pressure)	Pa
T_c	10		mK
P_c	15		Pa
e_s^{calc}	$44\times10^{-6}\, e_s^{calc}$		Pa
f_s^{calc}	$P_s/(10^7 \cdot \text{Pa})\ (18.3\ \text{K}/T_s - 0.047)$		--
e_c^{calc}	$44\times10^{-6}\, e_c^{calc}$	$T_c \geq 0$°C	Pa
	$A \times 10^{-6}\ e_c^{calc}$ *	$T_c < 0$°C	
f_c^{calc}	$P_c/(10^7 \cdot \text{Pa})\ (18.3\ \text{K}/T_c - 0.047)$		--
x_p	10		$\text{nmol}\cdot\text{mol}^{-1}$
$\dot{n}_s$	$5\times10^{-4}\, \dot{n}_s$	($\dot{n}_s \geq 7.5\times10^{-6}\ \text{mol}\cdot\text{s}^{-1}$)	$\text{mol}\cdot\text{s}^{-1}$
	$1\times10^{-3}\, \dot{n}_s$	($\dot{n}_s < 7.5\times10^{-6}\ \text{mol}\cdot\text{s}^{-1}$)	$\text{mol}\cdot\text{s}^{-1}$
$\dot{n}_p$	$5\times10^{-4}\, \dot{n}_p$		$\text{mol}\cdot\text{s}^{-1}$

*$A = 7.2 - 17.1\ T_c$/°C + 0.105 $(T_c$/°C$)^2$

FIGURE CAPTIONS

Fig. 1. Schematic representation of the hybrid humidity generator (HHG) in a) two-pressure mode and b) divided-flow mode.

Fig. 2. Photograph of the final saturator.

Fig. 3. Total expanded relative uncertainty U_r for the mole fraction generated by the HHG saturator using the two-pressure principle in a) 1-P mode and b) 2-P mode with P_s = 500 kPa. The black curve represents the total uncertainty, while the other curves show the contributions from individual uncertainty elements. Here, $U_r(x) = ku(x)/x$, where $k = 2$ and $u(x)$ is the standard uncertainty for x.

Fig. 4. Total expanded uncertainty U for the frost/dew point generated by the HHG saturator when used in a) 1-P mode and b) 2-P mode with P_s = 500 kPa. Here, $U(T_{FP/DP}) = ku(T_{FP/DP})$, where $k = 2$ and $u(T_{FP/DP})$ is the standard uncertainty for $T_{FP/DP}$. Also, P, e^{calc}, and f^{calc} each represent the combined contributions of their quantity from both the saturator and chamber (hygrometer).

Fig. 5. Total expanded relative uncertainty $U_r(RH)$ for the relative humidity calibrations using humid gas generated by the HHG flowing to an environment of temperature T_c = 20 °C and pressure P_c = 100 kPa; here, $U_r(RH)$ includes the uncertainty for the calibration of the hygrometer's external temperature probe. In the plots, the generator is used in 2-P mode and the saturator temperature is a) 20 °C and b) 1 °C. The relative humidity is varied by changing the saturator pressure.

Fig. 6. Total expanded relative uncertainty for the water mole fraction generated by the HHG when it is used in divided flow mode with a saturator pressure of P_s = 300 kPa. Here, $\dot{n}$

represents the combined uncertainty contributions from the wet gas and dry gas mass-flow rates.

Fig. 7. Total expanded uncertainty for the frost point generated by the HHG when it is used in divided flow mode with a saturator pressure of P_s = 300 kPa.). Here, f^{calc} represents the combined uncertainty contributions from both the saturator and chamber (hygrometer), and $\dot{n}$ represents the combined uncertainty contributions from the wet gas and dry gas mass-flow rates.

Fig. 8. Total expanded relative uncertainty $U_r(RH)$ for the relative humidity calibrations using humid gas generated by the HHG flowing to an environment of temperature T_c = 20 °C and pressure P_c = 100 kPa, where the generator is used in divided-flow mode. Here, $U_r(RH)$ includes the uncertainty for the calibration of the hygrometer's external temperature probe.

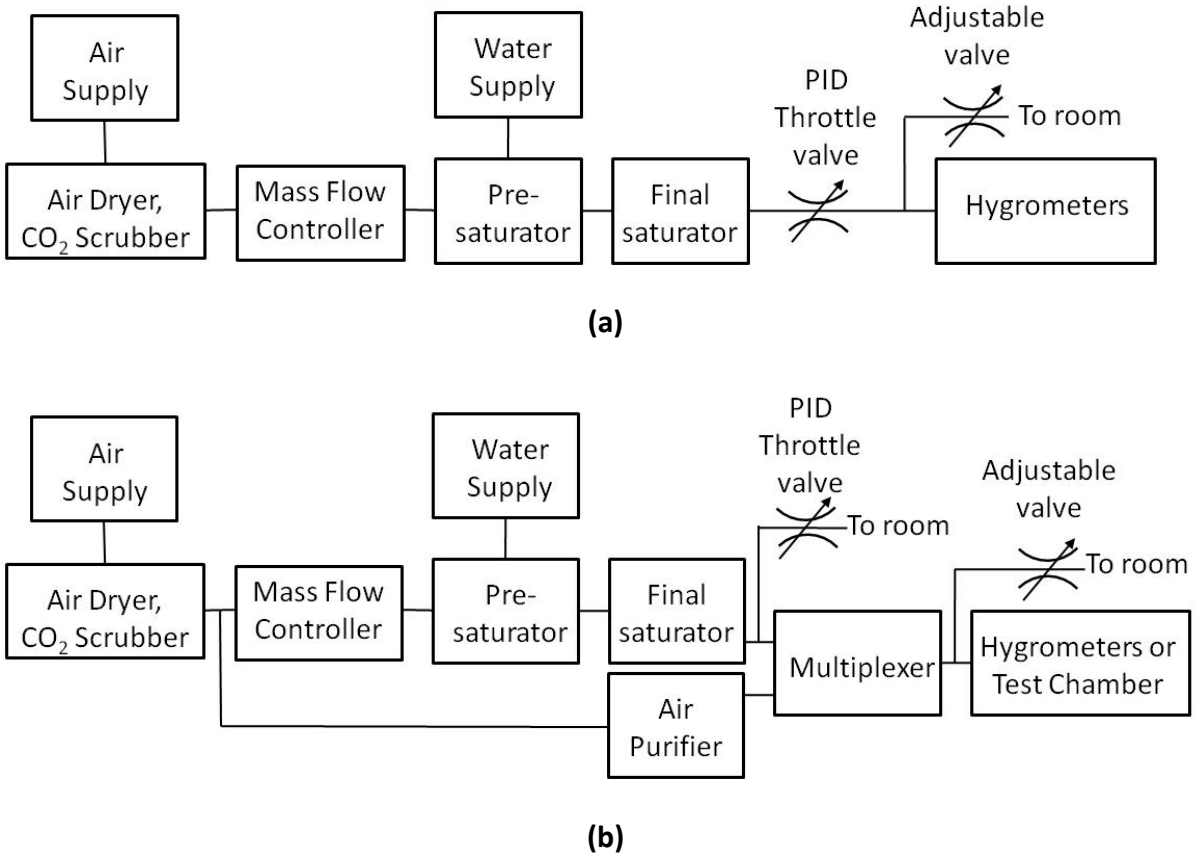
Air Supply
Air Dryer, CO_2 Scrubber
Mass Flow Controller
Water Supply
Pre-saturator
Final saturator
PID Throttle valve
Adjustable valve
To room
Hygrometers
(a)
Air Supply
Air Dryer, CO_2 Scrubber
Mass Flow Controller
Water Supply
Pre-saturator
Final saturator
PID Throttle valve
To room
Adjustable valve
To room
Multiplexer
Hygrometers or Test Chamber
Air Purifier
(b)

Figure 1

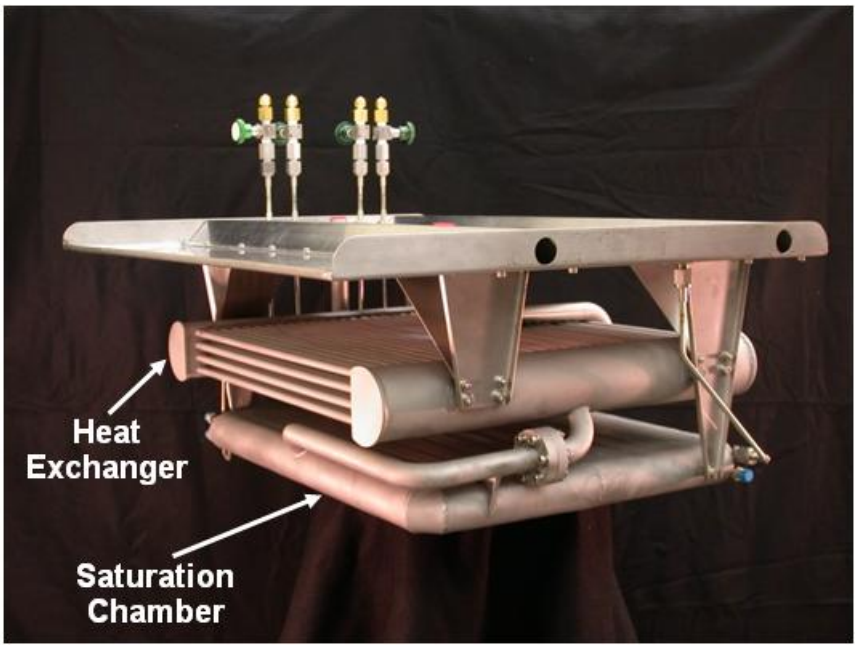

Figure 2

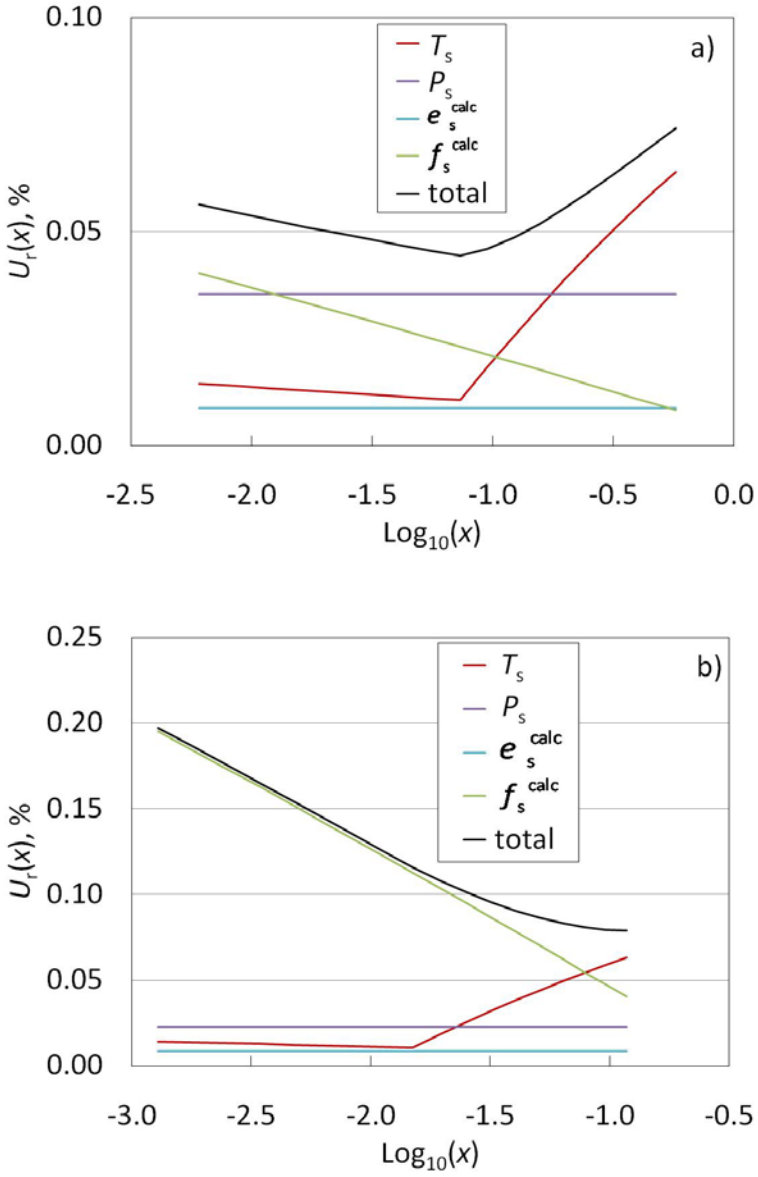
a)
T_s
P_s
e_s^{calc}
f_s^{calc}
total
$U_r(x)$, %
0.10
0.05
0.00
-2.5
-2.0
-1.5
-1.0
-0.5
0.0
$\mathrm{Log}_{10}(x)$
b)
T_s
P_s
e_s^{calc}
f_s^{calc}
total
$U_r(x)$, %
0.25
0.20
0.15
0.10
0.05
0.00
-3.0
-2.5
-2.0
-1.5
-1.0
-0.5
$\mathrm{Log}_{10}(x)$

Figure 3

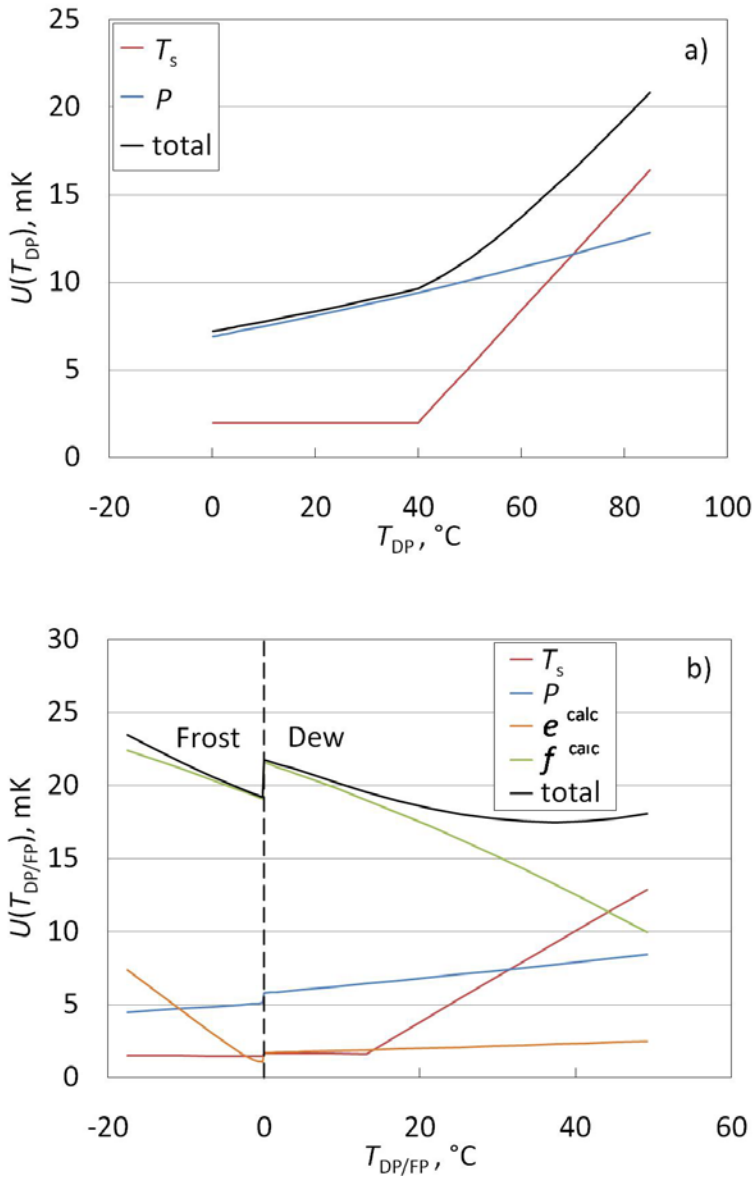
a)
T_s
P
total
$U(T_{DP})$, mK
T_{DP}, °C
b)
T_s
P
e^{calc}
f^{calc}
total
Frost
Dew
$U(T_{DP/FP})$, mK
$T_{DP/FP}$, °C

Figure 4

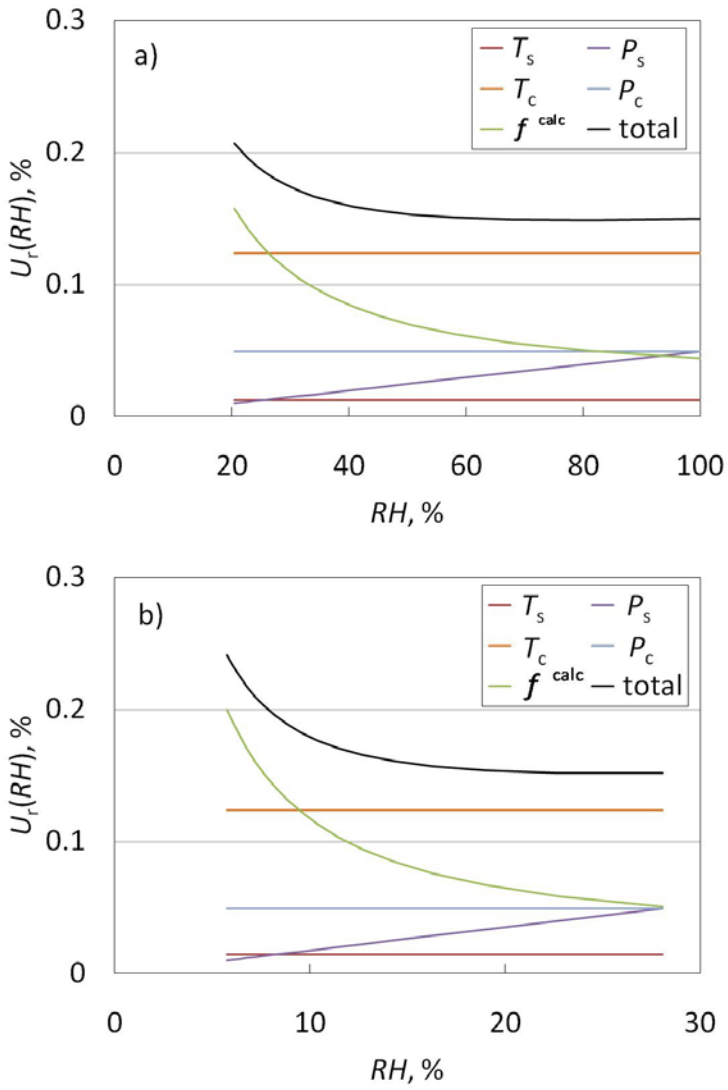
a)
T_s
P_s
T_c
P_c
f^{calc}
total
$U_r(RH)$, %
0.3
0.2
0.1
0
0
20
40
60
80
100
RH, %
b)
T_s
P_s
T_c
P_c
f^{calc}
total
$U_r(RH)$, %
0.3
0.2
0.1
0
0
10
20
30
RH, %

Figure 5

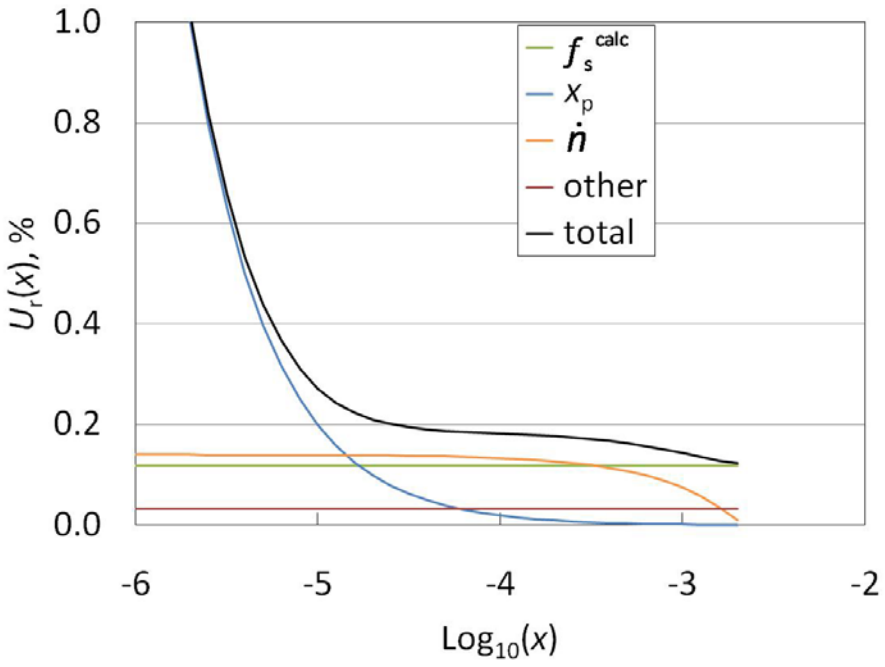
1.0
0.8
0.6
0.4
0.2
0.0
$U_r(x)$, %
-6
-5
-4
-3
-2
$\mathrm{Log}_{10}(x)$
f_s^{calc}
x_p
$\dot{n}$
other
total

Figure 6

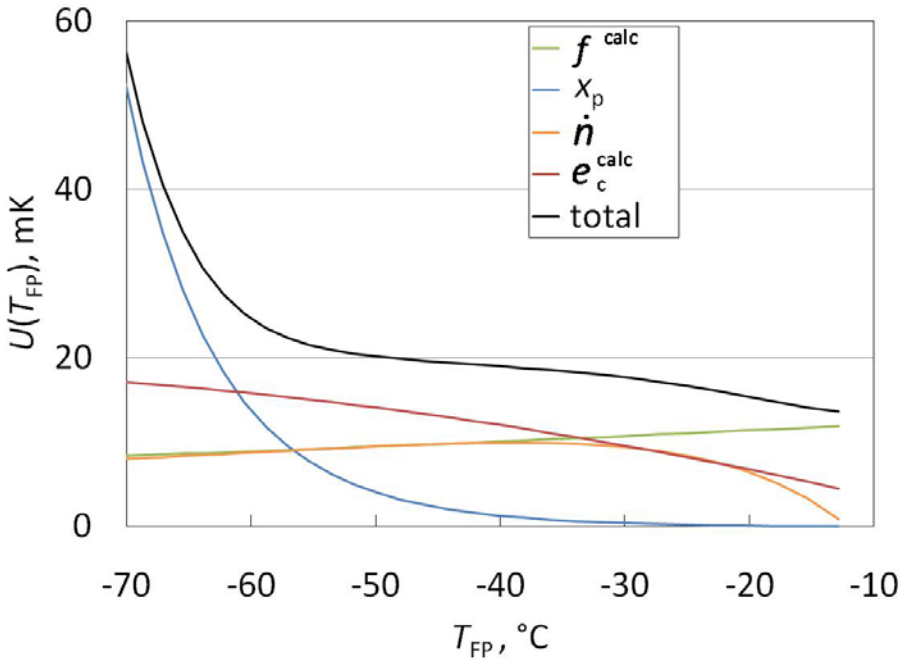
60
40
20
0
$U(T_{FP})$, mK
-70
-60
-50
-40
-30
-20
-10
T_{FP}, °C
f^{calc}
x_p
$\dot{n}$
e_c^{calc}
total

Figure 7

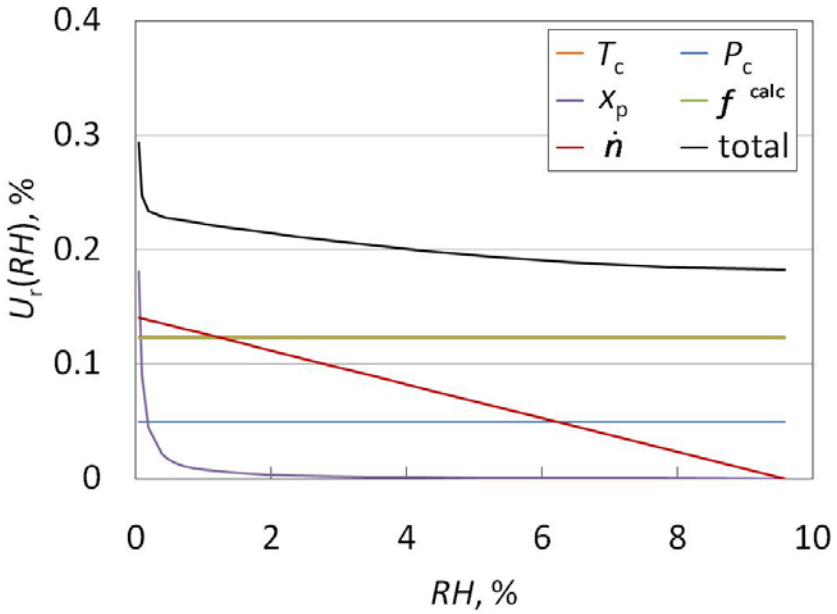

Figure 8